WHAT LIGHT?

or

THE QUESTION OF PARALLEL PUMPING IN FERROMAGNETS

by

Andrew Marcus Lear Kurn

B.A., Reed College, 1970

A THESIS SUBMITTED IN PARTIAL FULFILLMENT OF

THE REQUIREMENTS FOR THE DEGREE OF

MASTER OF SCIENCE

in the Department

of

Physics

SIMON FRASER UNIVERSITY

April 1977

APPROVAL

Name: Andrew Marcus Lear Kurn

Degree: Master of Science

Thesis Title: What Light? or The Question of Parallel Pumping in Ferromagnets

Examining Committee:

Chairman: Suso Gygax

J. F. Cochran
Senior Supervisor

E. D. Crozier

B. L. Jones

Bretislav Heinrich
University Examiner
Research Associate
Simon Fraser University

Date: 7 April 1977

PARTIAL COPYRIGHT LICENSE

I hereby grant to Simon Fraser University the right to lend my thesis or dissertation (the title of which is shown below) to users of the Simon Fraser University Library, and to make partial or single copies only for such users or in response to a request from the library of any other university, or other educational institution, on its own behalf or for one of its users. I further agree that permission for multiple copying of this thesis for scholarly purposes may be granted by me or the Dean of Graduate Studies. It is understood that copying or publication of this thesis for financial gain shall not be allowed without my written permission.

Title of Thesis/Dissertation:

What Light? or The Question of Parallel Pumping in Ferromagnets.

Author:

(signature)

Andrew M. KURN

(name)

21 April 1977

(date)

ABSTRACT

A brief introduction is given to the response of a ferromagnetic plate to monochromatic microwave radiation when it is subject to a constant magnetic field oriented parallel to the plate surface. A theory describing this response is presented which has a linear dependence on the amplitude of the incident radiation. The theory of Lieu and Alexandrakis for the case in which the microwave and static magnetic fields are parallel, which has a non-linear dependence on the amplitude, is shown to be in error.

Microwave transmission through a 40μm thick Supermalloy foil ($d/\delta = 22.5$) with RF and static magnetic fields parallel revealed a distorted replica of the perpendicular transmission signal, but attenuated 600-fold in amplitude. Transmission through a 7.2μm thick foil of nickel gave a field independent signal at fields greater than approximately 1 koe in agreement with the observations reported by Lieu and Alexandrakis. This background signal was found to be consistent in strength with that predicted by the theory described here. For both foils an extra transmission signal due to ferromagnetic domain walls was observed near zero static field.

But, soft! What light through yonder window breaks?
Romeo and Juliet II.2.1

I wish to extend my gratitude to Stephanie Cochran who provided the gerbils, to Doreen and Marion and Rick who fed the gerbils, to Maureen McIlmoyl for brute strength, to Wendell Bishop for a kind of low animal cunning, to John Cochran who provided advice, both good and bad, in heroic quantity, and to God who created all the above and invented magnetism to boot: the knight in His chessgame.

I am indebted to the members of our research group: Graeme Dewar, Bretislav Heinrich, and Rick Baartman whose brains I picked mercilessly. I am indebted to the National Research Council of Canada for funds which supported this work.

TABLE OF CONTENTS

LIST OF TABLES

LIST OF FIGURES

Mi ritrovai per una selva oscura,
Che la diritta via era smarrita.
Inferno I.1

Chapter 0

Introduction

Despite the fact that magnetism has been known since classical times, it has not been until this century that a quantitative theory has existed for permanent magnets. This is best ascribed to the fact that the mediating force is quantum mechanical in origin.

Condensed materials in which a magnetization arises spontaneously are called ferromagnets. If we take as a model the notion that a ferromagnet is made up of elementary magnets (avoiding the question of the source of the field, momentarily), it occurs to us that a magnetic dipole presents an aligning force to nearby dipoles and, therefore, we may explain this macroscopic magnetization in purely classical terms.

In fact, however, we know this not to be possible. Of the various sources of magnetic dipole moment, we know, at the atomic scale, that that intrinsic to the electron is the strongest. The energy associated with the alignment of neighboring electrons may be therefore compared with the energy associated with thermal excitations to show that no macroscopic alignment is possible above a few kelvins.

Instead we know that the familiar room-temperature magnetization is quantum mechanical in origin and has the scale of a coulomb interaction.

Moreover, the fact that the electron has spin ½ (intrinsic angular momentum $\frac{\hbar}{2}$) implies that its magnetic moment may be of no higher order than dipole and that this moment be parallel to the spin. (See, for instance, the derivation of (XIII.86) in Messiah (1962).)

Although the origin of the aligning force is known, its magnitude is not, since its evaluation involves an integral, the "exchange" integral which contains contributions from every electron in a macroscopic specimen. (See, however, some theoretical results by Hill and Edwards (1973).) Thus, this force constant, the exchange constant, lies in the realm of the empirical.

From the classical viewpoint, one may take the aligning field as a solely local magnetic dipole field (the Weiss field) of large magnitude. We can then make estimates of the strength of this field based on the susceptibility above the Curie temperature (based on the Curie-Weiss law) and the saturation magnetization below the Curie point (based on a Langevin function). (See for instance, Chapter 16, Kittel (1971).)

Unfortunately, we know from quantum mechanics (see, for example §10.11 Ziman (1972)) that the thermal excitation of a ferromagnet involves a large frequency spectrum of exchange coupled excitations (spin-waves). The study of ferromagnetic resonance (FMR) was undertaken to gain information about the response of a ferromagnet to monochromatic radiation. In particular, the exchange constant at low (microwave) frequencies is of interest.

A magnet with an associated angular momentum executes a circular precession when placed in a constant magnetic field. Although the effect is more complicated when the magnet is embedded in a metal (details to be found in the next chapter), there exists a precessional motion

in ferromagnets having a characteristic frequency. This precessional mode can be excited by microwaves as a resonance phenomenon, the frequency of which depends most strongly on the saturation magnetization, the applied external field, and the electron's gyro-magnetic ratio.

The theory I shall present in the next chapter follows that of Ament and Rado (1955) and Rado and Weertman (1959).

Since the position of the FMR line does not depend strongly on the exchange and the width of the line may or may not depend directly upon exchange (depending on the relative magnitude of the several damping mechanisms: The dependence is weak in Ni and Supermalloy, strong in Fe), it is desirable to have a method for measuring exchange reliably, independent of the other parameters of the material. Lieu and Alexandrakis (1975) claimed they had performed an experiment in good agreement with their theory which had a strong dependence on exchange. In this thesis I will show the error in their theory, I will show that the correct theory for their experimental configuration does not depend on exchange, and I will describe a similar experiment and compare the results I obtained with this theory.

In an external magnetic field, the best coupling to the magnetization of a ferromagnet is obtained if microwave radiation impinges on the sample polarized so that the microwave magnetic field is perpendicular to the magnetization. Lieu and Alexandrakis claimed, however, that a ferromagnet could be excited by microwaves polarized parallel to the magnetization. I will show that this is false (except at very high power levels) and that a ferromagnetic metal in this configuration responds chiefly as a metal with the familiar (μ=1) electro-magnetic fields in its interior, and not

as a ferromagnet.

Consider the lilies of the field, how they grow;
They toil not, neither do they spin.
Matthew 6.28

Chapter 1

Electromagnetic Waves and Spin Waves

Consider electromagnetic waves in vacuum. There are two degenerate eigenmodes of propagation for electromagnetic plane waves in a given direction. By degenerate, I mean that all waves of the same frequency have the same wavelength. Thus, one may choose a horizontal and vertical basis or a left and right-hand circular basis (or indeed among a continuum of other bases) *ad lib.*

In ferromagnetic metals there are four modes (as I will show below), which depend on the physical properties of the medium, two dependent chiefly on the conductivity σ, and two dependent chiefly on the ferromagnetic exchange constant A. The degeneracy is removed.

To be more precise: I shall consider a metal to be a classical continuum with a scalar (isotropic) local conductivity σ, such that $\vec{J} = \sigma \vec{E}$. Moreover, I shall assume that σ is large:

$$\epsilon \frac{\partial \vec{E}}{\partial t} \ll 4\pi\sigma\vec{E} \tag{1.1}$$

(All formulae are in cgs units.)

I shall consider a ferromagnetic metal to have the above properties

in addition to these: It has a non-zero magnetization $\vec{M}$ which has a fixed amplitude M_s (called the saturation magnetization), but not necessarily a fixed direction, everywhere in the metal. I will not make any mention of the temperature since it makes only quantitative (not qualitative) changes in a few parameters. The theory is applicable at any temperature low enough so that the amplitude of the magnetization is unperturbed by the applied field.

This magnetization is mediated by a "restoring force" with a coupling or elastic constant A called the exchange force, which tends to align the magnetization. If we model the energy of the magnetization at the origin

$$U = \vec{M}(0) \cdot \int \vec{M}(\vec{r})\, F(|\vec{r}|)\, d\vec{r}$$

and expand $$\vec{M}(\vec{r}) = \vec{M}(0) + (\vec{r} \cdot \nabla)\vec{M} + \cdots$$

we get $$\mathcal{U} = F_0 \vec{M}^2 + F_2 \vec{M} \cdot \nabla^2 \vec{M} + \cdots$$

With this in mind we take the form of the exchange torque to be

$$\vec{\tau}_{ex} = \vec{M} \times \frac{2A}{M_s^2} \nabla^2 \vec{M} \qquad (1.2)$$

which has the dimensions of a torque density $\frac{g}{\sec^2 \text{ cm}}$. This form of the torque equation is due to Herring and Kittel (1951). A is therefore in dynes $\frac{g \text{ cm}}{\sec^2}$. This exchange torque strongly evokes

the familiar

$$\vec{\tau} = \vec{M} \times \vec{B}$$

It is therefore tempting to speak in terms of an effective exchange induction. However, since $\vec{B}$ and $\vec{H}$ differ by a quantity parallel to $\vec{M}$, we may as easily speak in terms of an exchange field as an induction:

$$\vec{H}_{ex} \equiv \frac{2A}{M_s^2} \nabla^2 \vec{M} \tag{1.3}$$

The Laplacian has the effect of giving the difference between a sort of average value of $\vec{M}$ in the neighborhood and $\vec{M}$ itself. Thus, as long as A is positive, the exchange field will tend to align the magnetization parallel to the near-by magnetization. The magnetization in common ferromagnets arises chiefly (but see Argyres and Kittel (1953) for the contribution from the electron orbital motion) from the magnetic dipole moment of the electron. This moment follows the same rules and is always in the same state as the electron's intrinsic angular momentum, its quantum mechanical spin. Thus, we can define a positive γ such that

$$\vec{M} = -\gamma \vec{L} \tag{1.4}$$

where $\vec{L}$ is the classical angular momentum density due to spin. Both the angular momentum and the magnetization are at present thought to be fundamental to the electron and despite the suggestive names, no causal

relationship has been established between spin and magnetic moment. Nonetheless, the two terms are often used interchangeably, and, in particular, excitations which are coupled by the exchange field are called spin waves, to distinguish them from those coupled by the ordinary electromagnetic field. It should be emphasized that the exchange field is quantum mechanical in origin and is much stronger than the ordinary magnetic coupling of near-by spins. It arises from the Pauli exclusion of Fermions and in fact the term "exchange" comes from that context.

I shall deal with these geometries: Consider an infinite sheet of ferromagnetic metal with one surface passing through the origin. It will be infinite in the x and z directions with finite or infinite thickness towards +y. An rf EM excitation coming from the vacuum will have its magnetic field polarized along z. This excitation will be a plane-wave directed along y. A constant magnetic field will be applied either along x or z.

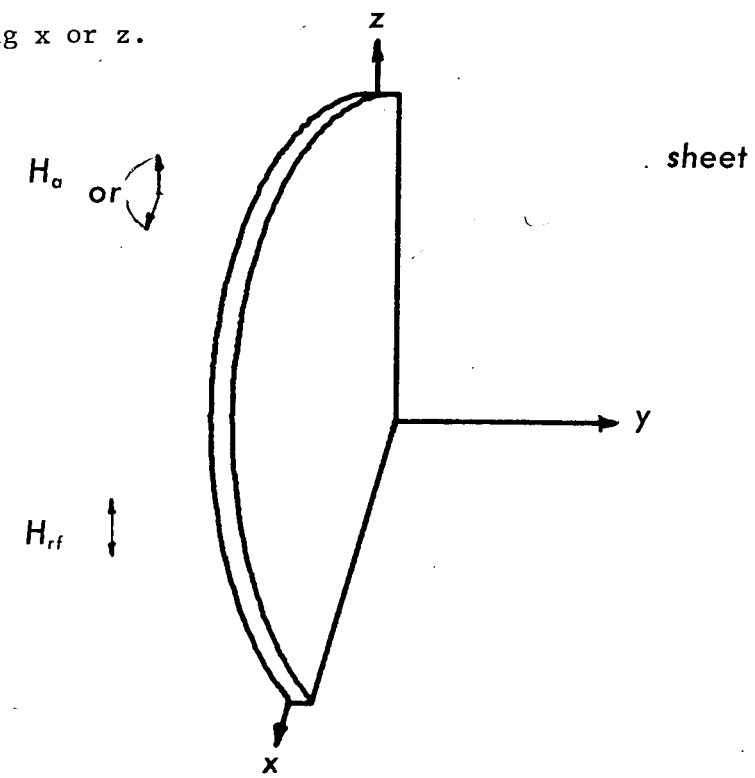

Since the DC field is always parallel to the slab surface, I will omit the term "parallel" as used by most authors from this chapter and use "parallel" and "perpendicular" to refer only to the relative orientation of the rf and DC magnetic fields.

I will first consider the perpendicular configuration.

Since we have a restoring torque (1.2) acting on an angular momentum (1.4) we expect precessional motion. I asserted at the outset that for a given frequency there would be four non-degenerate propagation vectors. For the approximation I adduce (1.1), Maxwell's equations are[1]

$$\nabla \cdot \vec{D} = 0 \qquad \nabla \times \vec{E} = -\frac{1}{c}\frac{\partial \vec{B}}{\partial t}$$

$$\nabla \cdot \vec{B} = 0 \qquad \nabla \times \vec{H} = \frac{4\pi\sigma}{c}\vec{E} \tag{1.5}$$

$$\vec{H} + 4\pi\vec{M} = \vec{B}$$

Following Lieu and Alexandrakis, I will use a propagator of the form

$$H_z = h_z e^{-(\lambda y + i\omega t)} \tag{1.6}$$

(Please note that λ is a wave-number in this work. Small letters

1. To see that $\nabla \cdot \vec{D} = 0$, note $\nabla \times \vec{H} = \frac{4\pi}{c}\vec{j}$ thus $\nabla \cdot \vec{j} = -\frac{\partial \rho}{\partial t} = 0$. For plane waves this implies $\rho = 0$.

will be used for amplitudes.) This yields (for plane waves)

$$B_y = 0 \qquad -\lambda e_z = \frac{i\omega}{c}(h_x + 4\pi m_x)$$

$$-\lambda e_x = -\frac{i\omega}{c}(h_z + 4\pi m_z)$$

$$E_y = 0 \qquad -\lambda h_z = \frac{4\pi\sigma}{c} e_x$$

$$-\lambda h_x = -\frac{4\pi\sigma}{c} e_z$$

Since $\vec{M}$ is of constant length and already oriented along x, any change in M_x is second-order in M_y and M_z. We can, in the limit of small signals, take $m_x = 0$. Thus we have

$$\lambda^2 h_z = -\frac{2i}{\delta^2}(h_z + 4\pi m_z) \tag{1.7}$$

but only

$$\lambda^2 h_x = -\frac{2i}{\delta^2} h_x \tag{1.8}$$

where I have defined the skin depth

$$\delta^2 \equiv \frac{c^2}{2\pi\omega\sigma}$$

Equation (1.8) represents an eigenmode of the medium uncoupled from the magnetization which we will therefore designate NM (non-magnetic).

$$\lambda_{AM} = \frac{\sqrt{-2i}}{\delta}$$

To find the solutions of (1.7) we need the torque equation relating H and M, this time containing both the exchange field (1.3) and the real field.

$$\vec{H}_{eff} = \vec{H} + \frac{2A}{M_s^2} \nabla^2 \vec{M} \tag{1.9}$$

Magnetic excitations in metals are chiefly damped by coupling to electron motion (spin-orbit coupling). Since the details of the damping do not interest us, it is convenient to introduce magnetic damping using a phenomenological relaxation time τ (Bloembergen damping). The introduction of damping in this particular form is merely to keep accord with Lieu and Alexandrakis. Using (1.4)

$$\frac{\partial \vec{M}}{\partial t} = -\gamma \vec{M} \times \vec{H}_{eff} - \frac{\vec{M}}{\tau} \tag{1.10}$$

So
$$-i\omega m_z = -\gamma M_s \left(-4\pi m_y + \frac{2A}{M_s^2}\lambda^2 m_y\right) - \frac{m_z}{\tau} + \gamma m_y H_a \tag{1.11}$$

$$-i\omega m_y = \gamma M_s \left(h_z + \frac{2A}{M_s^2}\lambda^2 m_z\right) - \frac{m_y}{\tau} - \gamma m_z H_a$$

where I have again dropped second-order terms and used $B_y=0$. Combining these gives

$$\frac{h_z}{m_z} = \frac{\left(\frac{1}{\gamma\tau} - \frac{i\omega}{\gamma}\right)^2 + \left(-\frac{2A}{M_s}\lambda^2 + H_a\right)\left[M_s\left(4\pi - \frac{2A}{M_s^2}\lambda^2\right) + H_a\right]}{M_s^2\left(4\pi - \frac{2A}{M_s^2}\lambda^2\right) + H_a M_s}$$

But from (1.7)

$$\frac{h_z}{m_z} = -\frac{8i\pi}{\lambda^2\delta^2 + 2i} \tag{1.12}$$

Thus

$$0 = \lambda^6 + \lambda^4\left(\frac{2i}{\delta^2} - \frac{M_s}{A}H_a - \frac{2\pi M_s^2}{A}\right) + \lambda^2\left[\frac{H_a^2 M_s^2}{4A^2} + \frac{\pi M_s^3 H_a}{A^2} - \frac{2iM_s H_a}{A\delta^2} - \frac{8i\pi M_s^2}{A\delta^2} + \frac{M_s^2}{4A^2}\left(\frac{1}{\gamma\tau} - \frac{i\omega}{\gamma}\right)^2\right] + \frac{4i\pi H_a M_s^3}{A^2\delta^2} + \frac{iH_a^2 M_s^2}{2A^2\delta^2} + \frac{8i\pi^2 M_s^4}{A^2\delta^2} + \frac{iM_s^2}{2A^2\delta^2}\left(\frac{1}{\gamma\tau} - \frac{i\omega}{\gamma}\right)^2 \tag{1.13}$$

This equation, being cubic in λ^2 contains the remaining three eigenvalues. We can readily see that only one exists in the absence of exchange since, as $A \to 0$, the equation becomes linear in λ^2.

Let me then examine this limiting case, and, subsequently, the limit in which spin waves dominate, to illuminate this initially opaque equation.

I define

$$B_a \equiv H_a + 4\pi M_s \tag{1.14}$$

$$\Gamma \equiv i\left(\frac{1}{\gamma\tau} - \frac{i\omega}{\gamma}\right) \tag{1.15}$$

The reason for my choice of phase for (1.15) is to make Γ mostly positive real, the relaxation time usually being long. In the no-exchange limit, then,

$$\lambda_{EM}^2 = -\frac{2i}{\delta^2}\,\frac{\beta_a^2 - \Gamma^2}{\beta_a H_a - \Gamma^2} \tag{1.16}$$

This is the so-called EM wave, the most interesting and experimentally accessible wave in the metal. It has potentially two interesting points: where the denominator goes through (near) zero and where the numerator does. Figures 1.1 and 1.2 represent the EM solution of the full equation (1.13) as a function of applied field. Both the real and imaginary parts are shown. It may be seen that if Γ is not large enough (i. e. if ω is not) with respect to M_s, the numerator may not go through (near) zero and the second of the resonant points will be missing. The point at which the denominator approaches zero is called ferromagnetic resonance (FMR). The point at which the numerator approaches zero is ferromagnetic anti-resonance (FMAR). Although it may seem clear that both of these points are of interest, the importance of FMAR (indeed its existence) was not well known until pointed out by Heinrich and Meshcheryakov (1969, 1970). At FMAR the damping is least, the skin depth is greatest, and there is a consequent transmission maximum. It is common to fix the frequency of the radiation and slowly sweep the applied magnetic field. In this case there is a specific field corresponding to FMR and (if a sufficiently high frequency is chosen) another corresponding to FMAR. It goes without saying that during transmission experiments, FMAR is the important point. A patient inspection of Figures 1.1 and 1.2 (a solution of the full secular equation (1.13)) reveals that

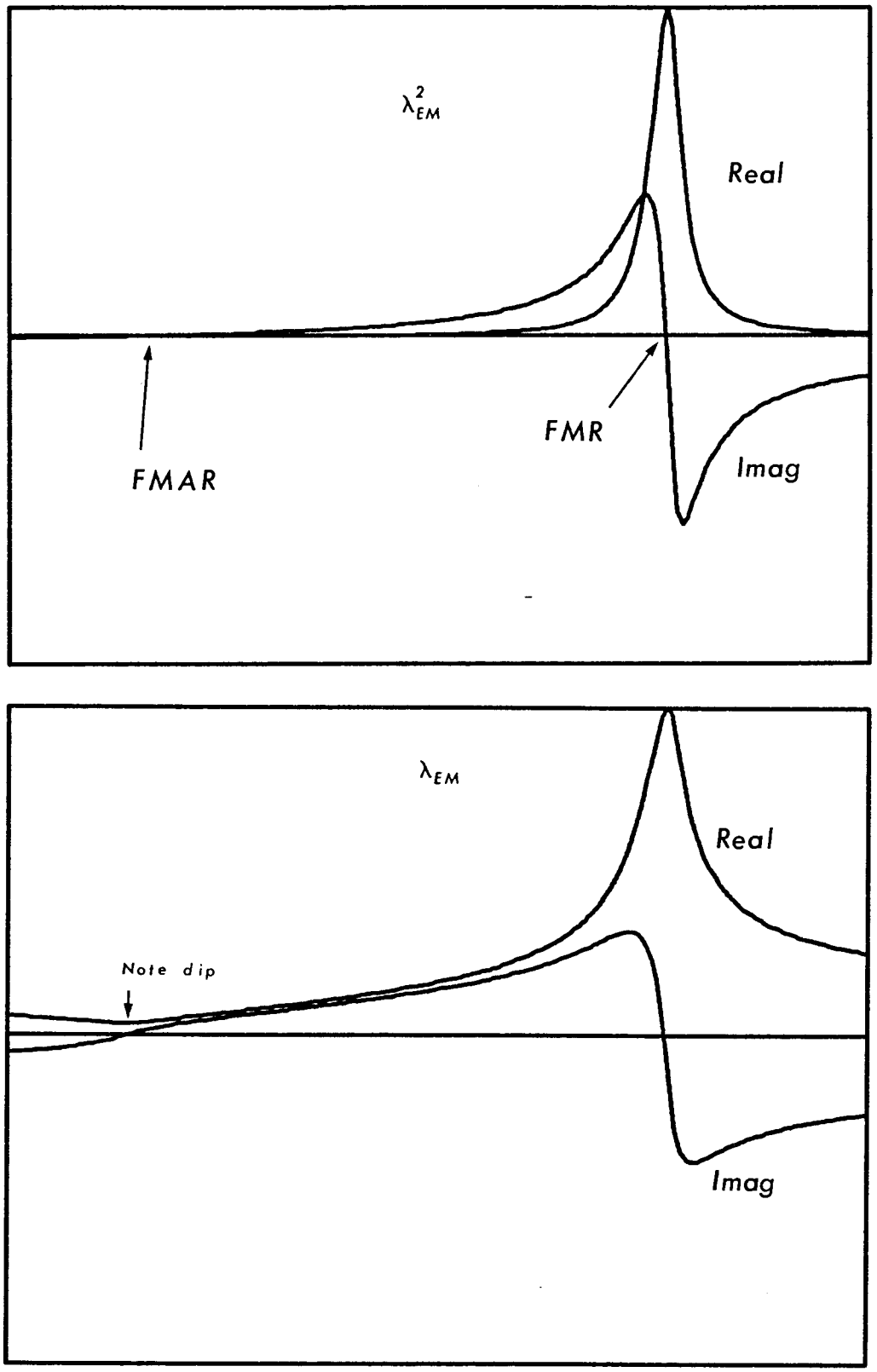

Figure 1.1 Propagation constant for the EM wave as a function of magnetic field.

although there is simple linear behavior in λ^2 at FMAR, there is a dip in the real (damping) part of λ. Moreover, since λ appears in an exponential (1.6), the effect of a small decrease in the real (damping) part of λ is greatly accentuated in any signal appearing at the back surface of the slab.

Now let me turn my attention to the spin waves. Intuitively, these are the solutions of the torque equation (1.10) without reference to the consequent to Maxwell's equations (1.7), i. e. where the short-range exchange force dominates. The easiest way to do this is in (1.11) to set the magnetic field h to zero. This gives

$$\left(\frac{1}{\gamma\tau} - \frac{i\omega}{\gamma}\right) m_z = \left(4\pi M_s - \frac{2A}{M_s}\lambda^2 + H_a\right) m_y$$

$$\left(\frac{1}{\gamma\tau} - \frac{i\omega}{\gamma}\right) m_y = \left(\frac{2A}{M_s}\lambda^2 - H_a\right) m_z \qquad (1.17)$$

So

$$\left(\frac{1}{\gamma\tau} - \frac{i\omega}{\gamma}\right)^2 - \left(\frac{2A}{M_s}\lambda^2 - H_a\right)\left(4\pi M_s - \frac{2A}{M_s}\lambda^2 + H_a\right) = 0$$

If I define

$$B_a \equiv H_a + 4\pi M_s \qquad (1.14)$$

$$\left(\frac{1}{\gamma\tau} - \frac{i\omega}{\gamma}\right)^2 + B_a H_a - (H_a + B_a)\frac{2A}{M_s}\lambda^2 + \frac{4A^2}{M_s^2}\lambda^4 = 0$$

the solution of which is

$$\lambda^2 = \frac{M_s}{4A}\left[(H_a + B_a) \pm \sqrt{(4\pi M_s)^2 - 4\left(\frac{1}{\gamma\tau} - \frac{i\omega}{\gamma}\right)^2}\right] \qquad (1.18)$$

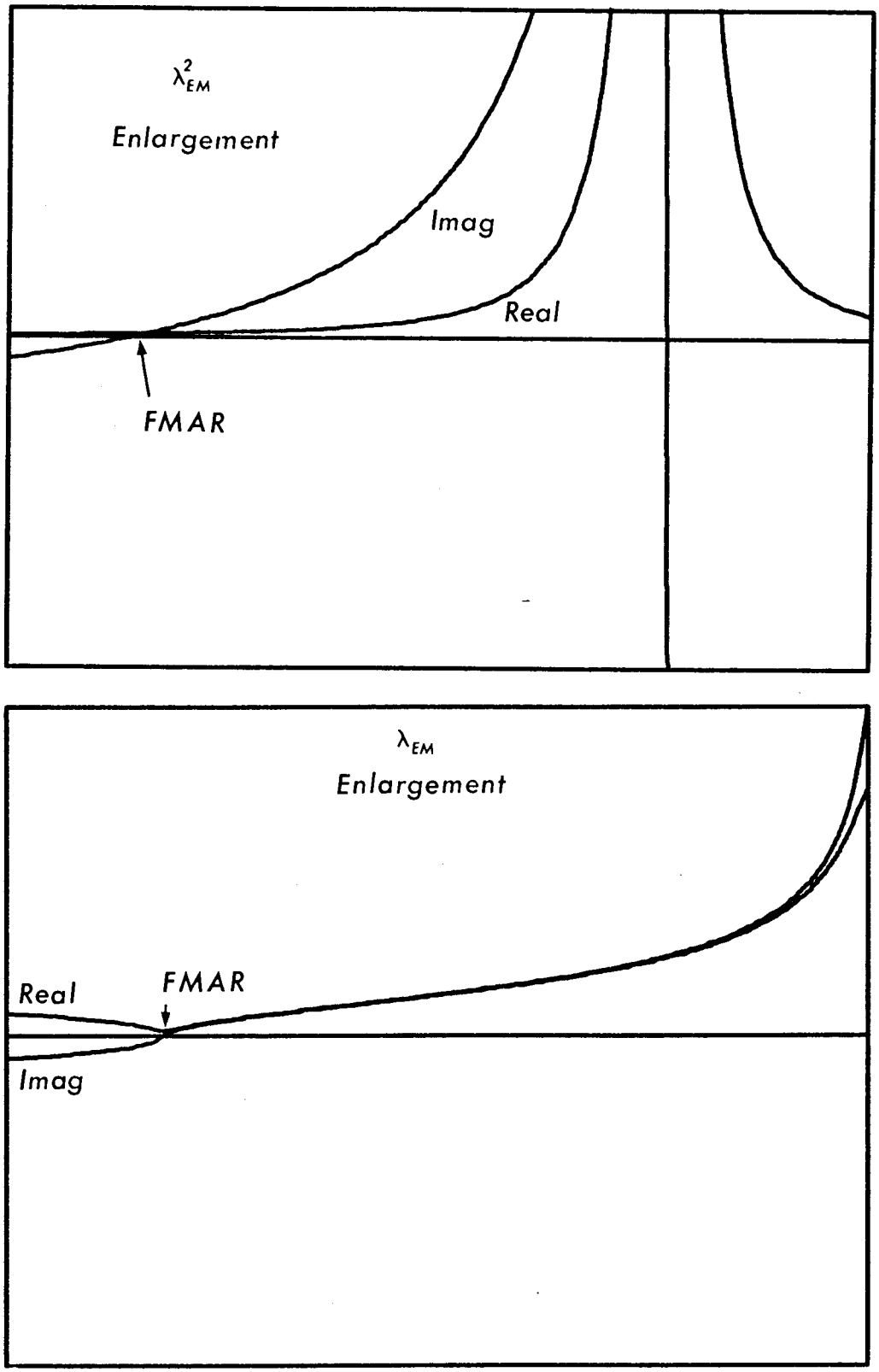

Figure 1.2 Enlargement of FMAR region of Figure 1.1. Damping has been reduced in the lower graph.

One sees quickly that λ^2 is linear with field. One of the roots is large and positive everywhere and therefore strongly damped and uninteresting. The other has a zero crossing at

$$\left(\frac{1}{\gamma\tau} - \frac{i\omega}{\gamma}\right)^2 + \beta_a H_a = 0$$

or

$$\beta_a H_a - \Gamma^2 = 0 \qquad (1.19)$$

in the limit of large τ, the relaxation time. Thus this root also has interesting behavior at FMR (see Figure 1.3). It should be added, however, that typically this wave has a λ that is quite large: of the order of $\frac{100}{\delta}$. This causes it to be largely unexcited at the interface, the λ for vacuum being nearly zero.

All three solutions are largely unperturbed when they are combined into the full secular equation, as may be seen from the fact that, although the figures are actual solutions of the full equation (1.13), they represent quite well the behavior of the limiting cases (1.16, 1.18). The only point at which mixing of solutions begins to occur is at the applied field corresponding to FMR, when the spin-wave comes down toward zero and the EM wave goes through a localized maximum. However, since our present interest is in FMAR, I will not explore the detailed solution of equation (1.13) any further.

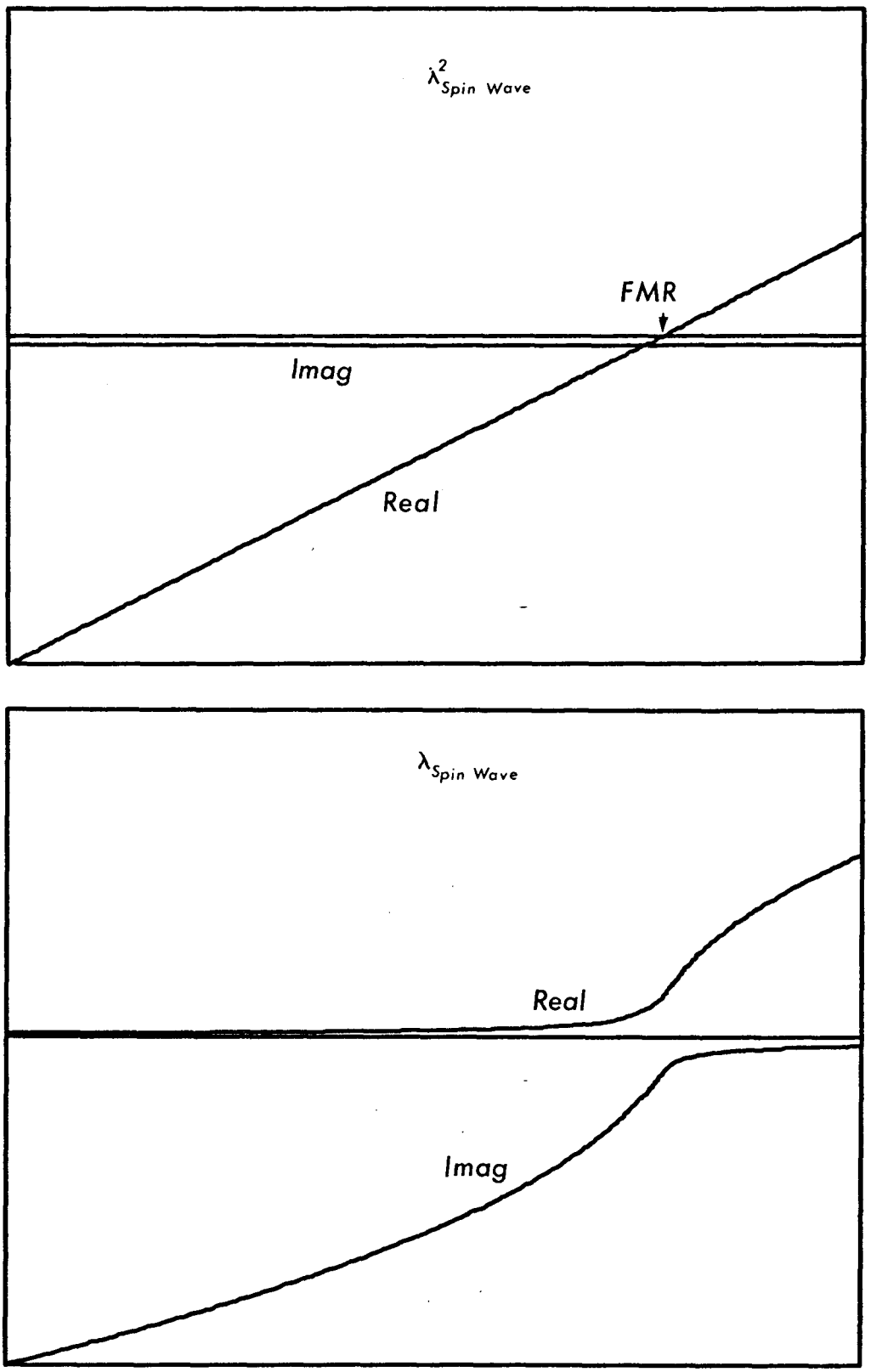

Figure 1.3 Propagation constant for the active spin wave as a function of magnetic field.

Yet in thy dark streets shinith
The everlasting light.
"O Little Town"
Bishop Phillips Brooks

Chapter 2

The Allegation of Lieu and Alexandrakis

I'd like to turn now to the precessional motion. Although I may

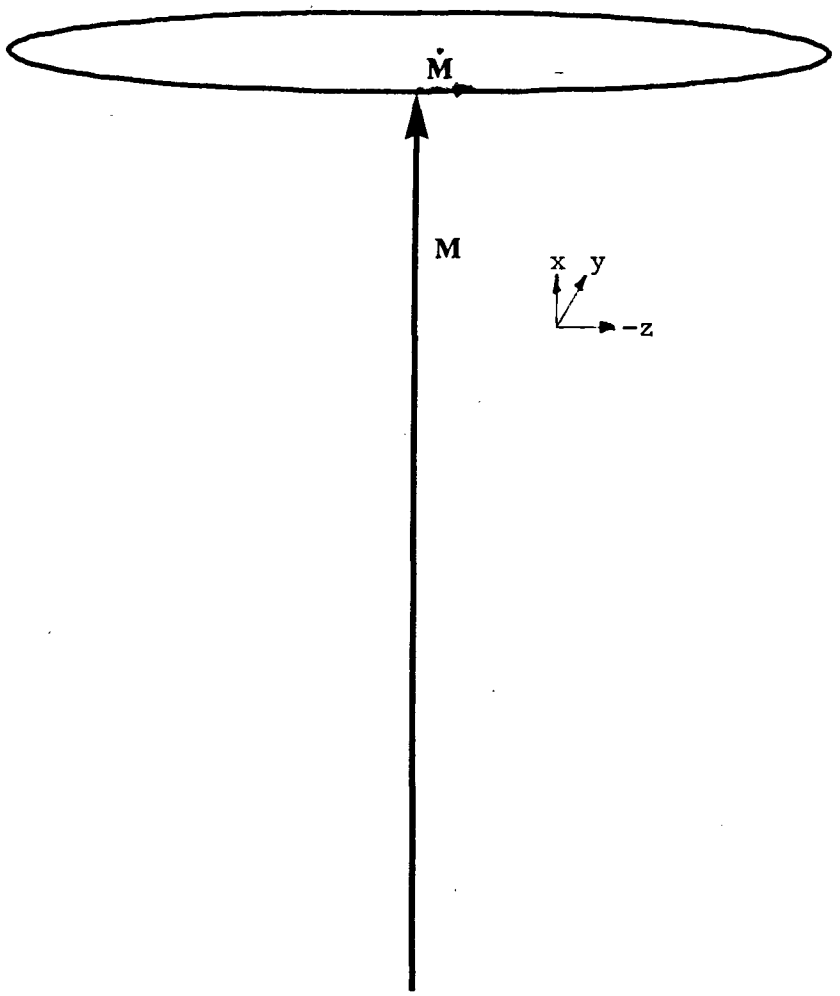

Figure 2.1 The precession of the magnetization.

have misled you while I was speaking of a magnetization precessing in an external field, there is no *a priori* reason for the excursion of the magnetization to be circular. The complete torque equation (1.10) contains several terms, and the presence of boundaries in the y-direction

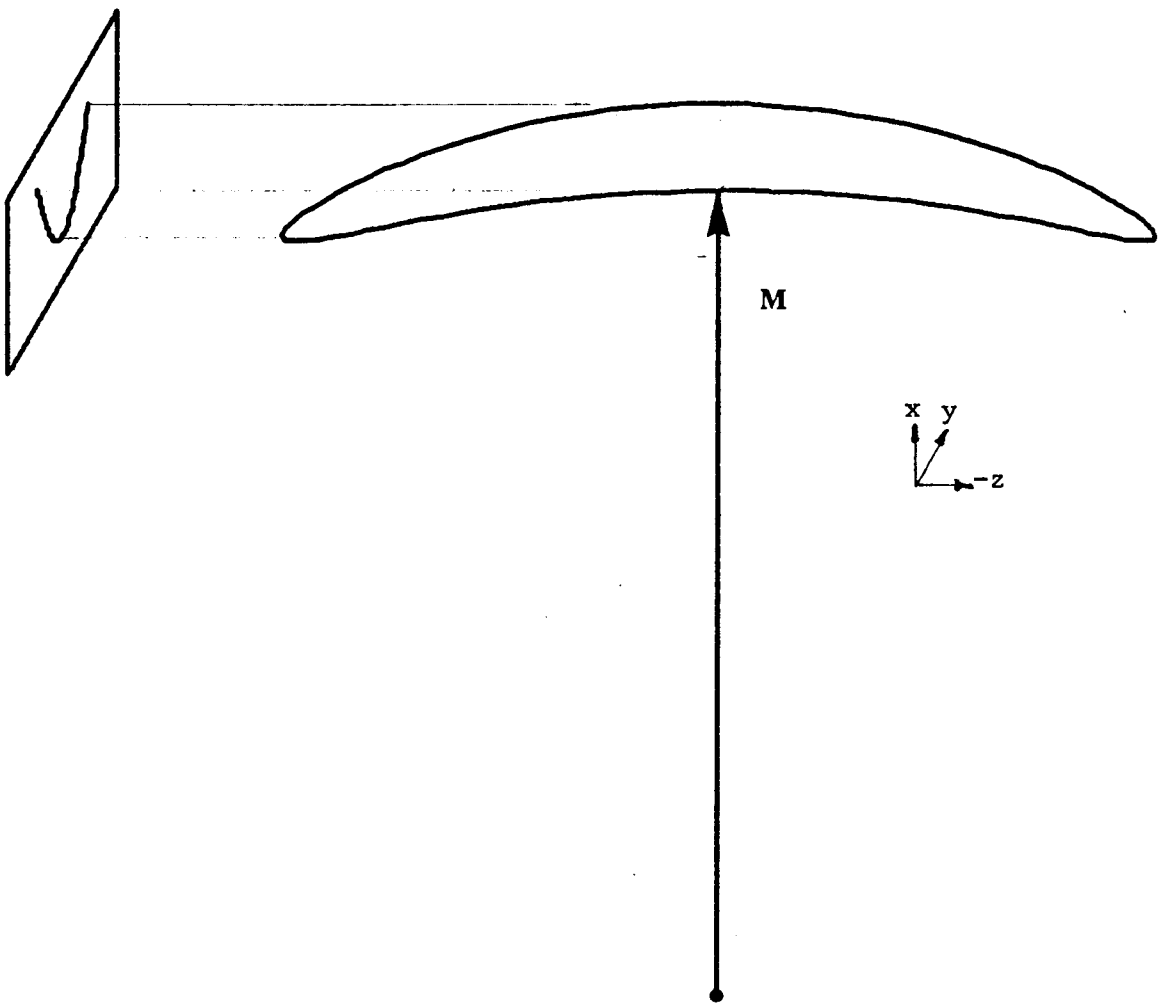

Figure 2.2 An elliptical precession of the magnetization displaying non-linearity in the presence of a large excitation.

with the consequent build-up of surface magnetic charge[1] is an adequate reason in general for an elliptical excursion as pictured in Figure 2.1. In this figure and the next, we look in the direction of +y towards the sample surface. The constant magnetic field is applied along x. Since the magnetization is fixed in amplitude, it becomes clear that this excursion can cause a second-order change in M_x as in Figure 2.2, i. e.,

$$M_x = \sqrt{M_s^2 - M_y^2 - M_z^2} \cong M_s \left(1 - \frac{M_y^2 + M_z^2}{2M_s^2}\right) \quad (2.1)$$

Now without stretching your credulity too far, I believe I can state, without yet resorting to mathematics, that this small change in M_x can be used to excite any elliptical (not circular) precessional mode. Consider the steady state. If there is an alternating magnetic field in the x-direction at twice the precessional frequency, it will clearly transfer energy to a precessing dipole. Since the amount of energy transferred ($\Delta E = B_x \Delta M_x$) itself depends upon ΔM_x, the energy transfer follows an exponential growth or decay law. Thus we see that there is a threshold for the exciting field, below which the dipole will relax to rest.

This coupling, where the exciting field is parallel to the static field, is what is commonly called parallel pumping. In due course, it was observed in an insulator (YIG) at sufficiently large rf fields ($\sim$1 oe) by Schlömann et al. (1960). This field can be easily shown

1. I am speaking here in analogy with the electrostatic case. By magnetic charge, I mean $\nabla \cdot \vec{H} = -4\pi \nabla \cdot \vec{M}$

to correspond to 1.2×10^9 erg/cm^2-sec (120 watt/cm^2) in free space. We (1976) have calculated the threshold for the appearance of parallel pumping in nickel to be ~ 85 oe corresponding to 8.7×10^{12} erg/cm^2-sec.

Lieu and Alexandrakis (1975, reproduced as the Appendix) reported an experiment and theory reminiscent of parallel pumping in metals at much lower power levels. They present a theory which predicts an excitation of the magnetization for low power levels in the parallel configuration. As a function of field, the amplitude they expect is shown in Figure 2.3. They observed a transmission qualitatively similar to this. Their theory runs as follows.

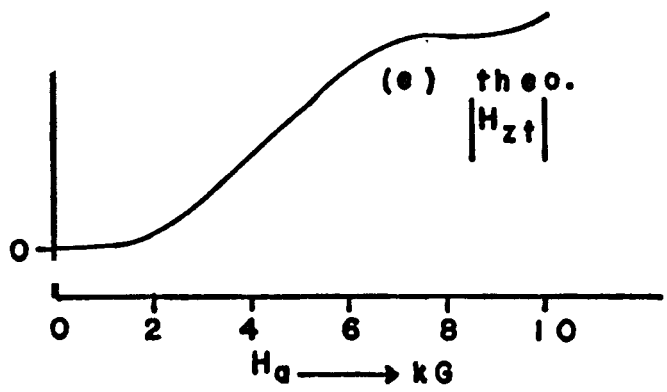

Figure 2.3 Lieu and Alexandrakis' theoretical results for nickel.

They start much as I have by adducing Maxwell's equations (1.5) and the torque equation (1.10). They also write the component of the torque parallel to the magnetization, a second-order term. These comprise their equations (1). They do not, however, use the longitudinal torque equation when deriving their solution for the wave-number (2). Hence, the solution they get is identical to (1.13). They next take the trouble to write the magnitude of the longitudinal disturbance in terms of the amplitudes of the three transverse ones. They next state that they will use 10 boundary conditions. Forming equations (5) are 6 of them, while the other 4 are equations (8). It is crucial to realize that they solve just 10 boundary conditions.

Let me recapitulate, but this time speaking only of one surface, so that the number of wave amplitudes and boundary conditions is cut in half.

They solve for the propagation vectors of wave-like disturbances in the magnetization. Since they ignore the fields at that point, they miss the solution which leaves the magnetization unexcited, the one I called λ_{NM}.

Since one mode is missing from the metal, it follows that, to be soluable, the boundary value problem must be changed. Let me show that the problem as originally stated required 6 conditions: Consider a semi-infinite sample so that we need deal only with the first surface. Consider that the general monochromatic wave is incident upon it, so that an amplitude is needed for each of the polarizations. These

two amplitudes are given. We must fix the amplitudes of the 2 reflected waves and those of the 4 waves inside the metal. We have immediately the boundary conditions on $E_{x,y}$ and $H_{x,y}$ from classical electrodynamics. For the remaining 2 conditions, we must turn to Rado and Weertman (1959). Their general treatment allows of three limiting cases of which $m_{x,y}=0$ is a common choice (Kittel's condition). However, the form of the boundary conditions is not crucial to my argument at this point. What is crucial is that there necessarily be 2 conditions, of whatever form.

This may be argued in the following manner. Recall that the magnetization has an associated angular momentum. The excitation of a sample involves the application of torque by one interior elementary magnet upon the others. The environment of the surface layer magnets is different from those in the bulk. Thus, the torque on these is going to be different from the others. In general, there are three components of torque, but since $M_z = M_S$ acts as a constraint, only two conditions on $\vec{M}$ are necessary.

I have shown that 6 boundary conditions exist. I have said that Lieu and Alexandrakis solved for only 5 wave amplitudes. To succeed at this, they ignored one of the boundary conditions, to wit, $m_y=0$ (when deriving their equation (5)). That their problem yields a non-zero solution at all depends on these matching errors.

God said to Abraham,
"Kill me your son."
Abraham said, "You must be
Putting me on!"
God said, "No!"
Abe said, "Why?"
God said, "you can do what you
Want, Abe, but the
Next time you see me coming,
You'd better run!"

"Highway 61"
Bob Dylan

Chapter 3

The Experiment

Lieu and Alexandrakis report at the same time as they presented their theory, results of transmission experiments on iron and nickel foils. These both have the property that they rise from zero amplitude (in the presence of no applied magnetic field) to a fairly flat plateau above a few kilogauss. In the experiments I performed, there also appeared a flat plateau above a few kilogauss. However, here, the transmission fell to this value rather than rose. Both of these observations are in basic agreement with the predictions made above of a non-magnetic mode, but modulated near zero field by the motion of ferromagnetic domain boundaries.

EXPERIMENTAL DETAILS

The 24 GHz transmission system used for these experiments was developed and debugged by J. F. Cochran and B. Heinrich to whom I

gratefully acknowledge my debt. It is described more fully elsewhere (Cochran et al. (1977a)). The specimens in the form of thin discs (see Table 3.I) were clamped between identical critically coupled transmitter and receiver cavities, so that the specimen formed one end-wall of each cavity. (See Figure 3.1) The rf magnetic fields of the TE_{10} mode

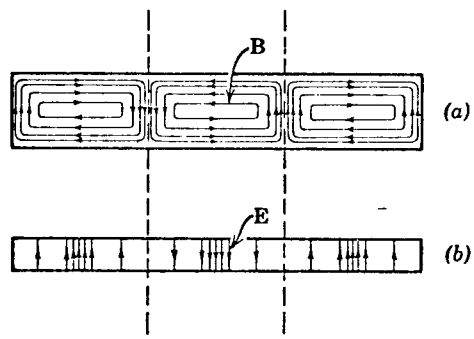

Figure 3.1a Fields inside an ideal resonant cavity.

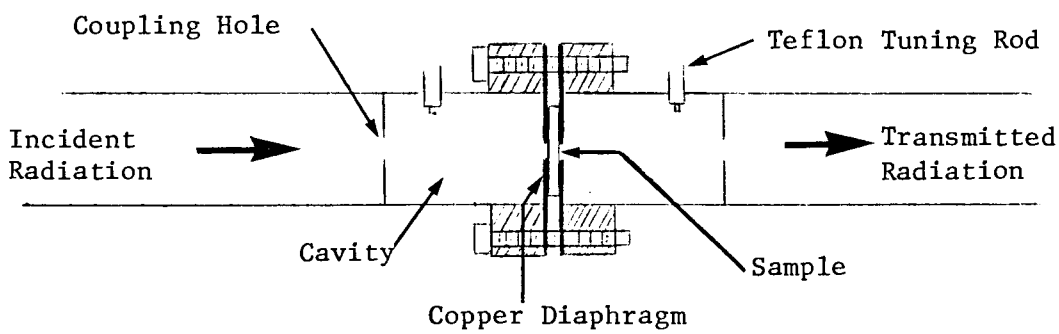

Figure 3.1b Cavities and sample from the 24 GHz transmission system.

Table 3.I Properties of the Supermalloy and Nickel used in this work. $\delta^2 = \rho c^2/2\pi\omega$ is the square of a scaling length, where ρ is the resistivity in esu. The demagnetizing field in the specimen is given by $H_D = 4\pi D_x M_s$.

Table 3.I

SPECIMEN	D Diameter cm	d Thickness μm[c]	$\frac{d}{D}$	D_x^d
Supermalloy[a]	1.6	40	2.5×10^{-3}	1.96×10^{-3}
Nickel[b]	1.0	7.2	7.2×10^{-4}	5.65×10^{-4}

SPECIMEN	ρ in μΩ cm at 26°C	d/δ	Iris area mm^2	$4\pi M_s$ (koe)[e]	ω/γ (koe)[e]
Supermalloy[a]	59.8	15.9	2.0	7.38	8.14
Nickel[b]	7.8	7.9	.4	6.06	7.85

a) Obtained from Perfection Mica Co. under the trade name Conetic AA. (740 Thomas Drive, Bensenville, Ill., 60106)

b) Goodfellow Industries Ltd., Ruxley Towers, Claygate-Esher, Surrey, England. 99% pure, the chief impurities were Fe and Co.

c) Thicknesses were calculated from the weight and area of the specimens.

d) Calculated for the appropriate ellipsoid of revolution.

e) Measured in our laboratory for similar material. See Cochran et al., (1977a) and Dewar et al. (1977).

in each cavity were parallel. The unloaded Q of each cavity was approximately 1500. Approximately 300 mw of power was incident upon the transmitter cavity, and the receiver had a sensitivity of 10^{-18} watts using a time constant of 1.25 seconds. The cavities were suspended between the poles of a Varian V-3800 15" electromagnet. The magnet could be rotated around a vertical axis such that the magnetic field remained parallel with the specimen plane within 1-2°. All measurements were carried out on unannealed foils at room temperature, approximately 26°C.

Relevent characteristics of the two specimens used for the present experiments are listed in Table 3.I. Discs were machined from the rolled foil by sandwiching the foil between flat pieces of stock; in this way it was possible to produce discs without burred edges. The nickel disc was used without further polishing; the Supermalloy disc was electropolished to produce a shiny surface (Bloembergen (1950)). Transmission through each specimen was limited to an area of a few mm^2 near its center by means of an evaporated gold layer 5-10 μm thick. It was hoped in this way to minimize the non-homogeneity of the TE_{10} rf driving field, and to minimize the effect of spatial inhomogeneities in the static magnetization caused by demagnetizing fields generated at the edges of the disc.

Leakage of microwave radiation around the specimens was negligably small for all experiments reported below[1]. This could be checked by sweeping the external magnetic field through ferromagnetic resonance

1. In the case of the Ni foil it was found necessary to seal the cavities using conducting silver paint as described by Cochran et al. (1977a).

in the orientation corresponding to orthogonal rf and static fields (the parallel-perpendicular configuration). It is the experience of our group that for thick specimens, such as those used here, any leakage of radiation around the specimen results in a field dependent signal at FMR (because of the modulation of the surface impedence). A small field-independent background signal ($\sim 10^{-15}$ watts) is always present in our apparatus due to direct leakage between the transmitter and receiver wave-guide systems (primarily leakage through the microwave switches used to tune the cavities and to calibrate the receiver sensitivity). This field independent background signal was measured at the external field corresponding to FMR with the field oriented in the parallel-perpendicular configuration. The background signal was subtracted from the raw transmission data, having due regard for its phase. Transmission signals having this background subtracted are reported below.

RESULTS

In our experimental system, transmission amplitude is measured as a function of magnetic field for two orthogonal phases. The digitized data for the two phases are then combined to give the transmission amplitude and the field dependence of the phase. The results of an experiment on the Supermalloy disc for the parallel-parallel configuration are shown in Figure 3.2. The large amplitude variation shown in Figure 3.2 was due to a residuum of the FMAR signal: the transmission peak was approximately 600 times weaker than the FMAR signal observed for the parallel-perpendicular configuration (see Figure 3.3). The

Figure 3.2 Tracings of the transmission signals observed for the 40 μm thick Supermalloy disc using the parallel-parallel configuration (rf and static magnetic fields parallel). Two orthogonal phases are shown; these data were combined to give the transmission amplitude vs. field shown in Figure 3.4. The maxima correspond to a residuum of the usual FMAR signal. This residual FMAR signal corresponded to a peak power of approximately 10^{-15} watts for an incident power of 1/3 watt. The bandwidth of the system was limited by an output time constant of 1.25 seconds.

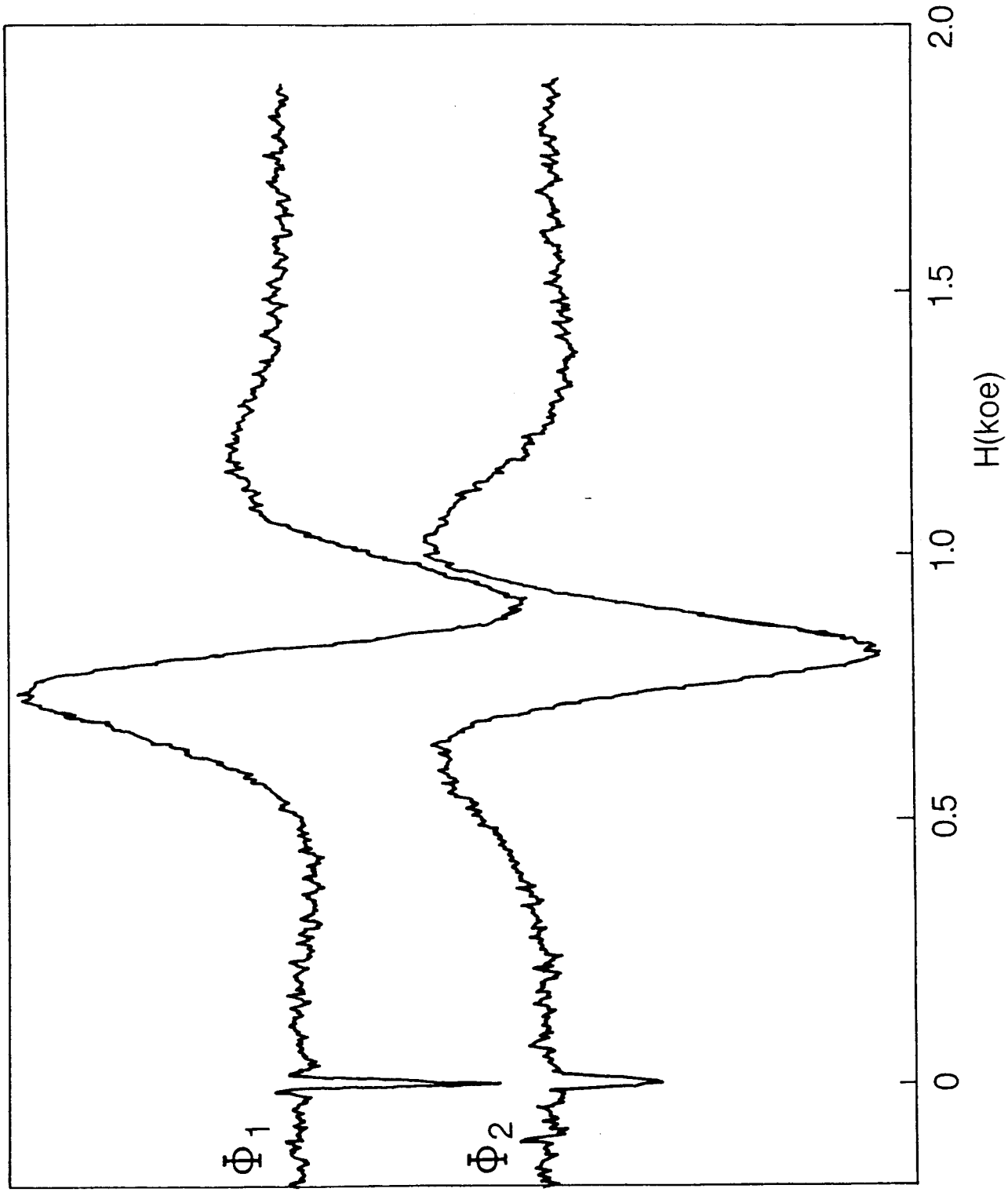
Φ_1
Φ_2
0
0.5
1.0
1.5
2.0
H(koe)

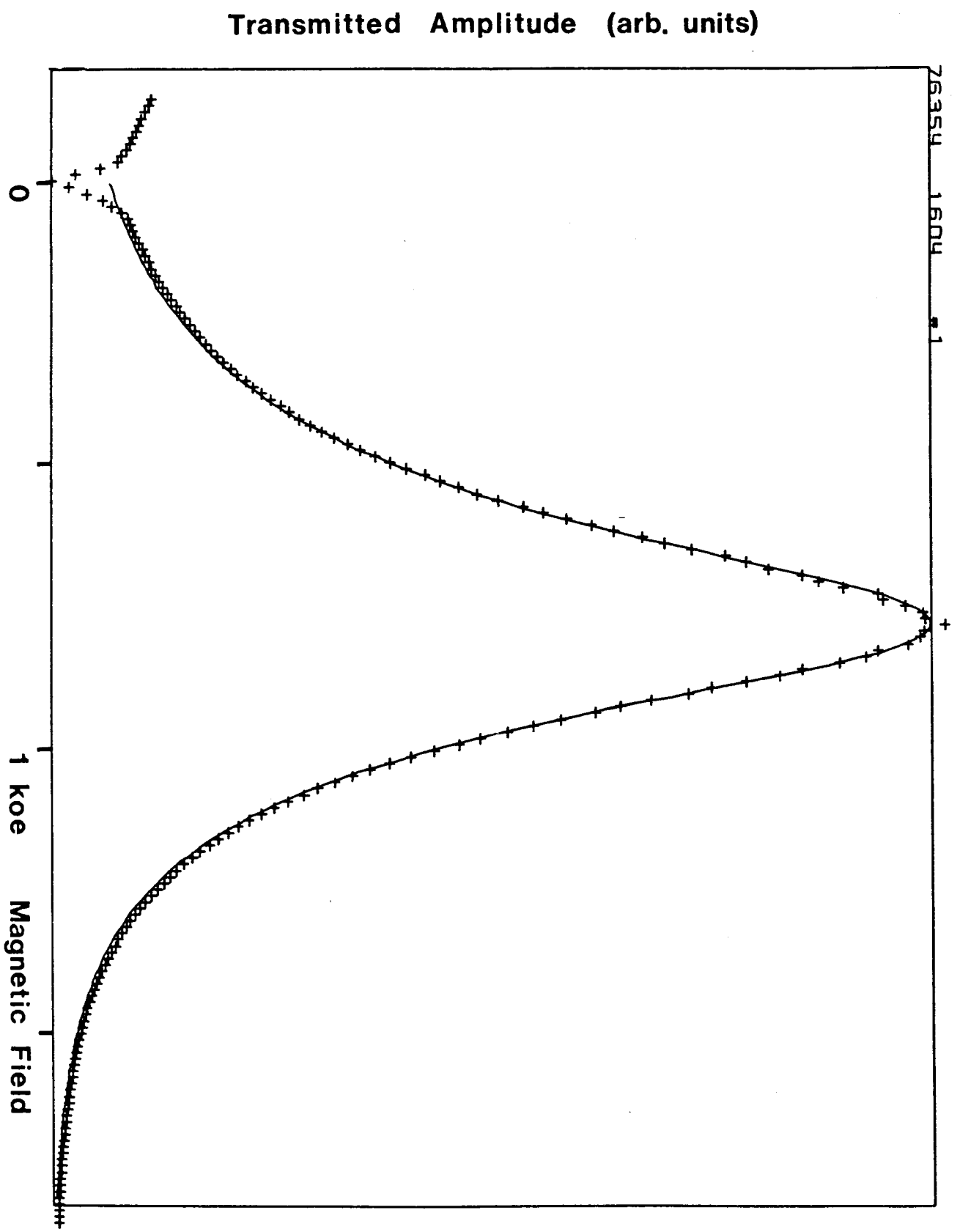
Transmitted Amplitude (arb. units)
0
1 koe
Magnetic Field
76354 1604 #1

Figure 3.3 Transmission amplitude vs. magnetic field strength for the 40 μm thick Supermalloy disc using the usual parallel-perpendicular FMAR configuration. The peak signal corresponded to a power transmission ratio of -91 db. It occurred at 0.78 koe. The solid curve was calculated using the parameters listed in Table 3.I and a Landau-Lifshitz damping parameter of 1.15×10^8 Hz.

amplitude of the noise on the signals shown in Figure 3.2 corresponds approximately to 10^{-18} watts. Of particular interest are the transmission spikes which occurred near zero field. These transmission spikes were bounded by approximately ±15 oe on either side of zero field, and were due to the presence of domain boundaries in the specimen[2]. The value 15 oe for the departure field obtained from the data of Figure 3.2 agrees well with the value $4\pi M_s D_x$ = 14.5 oe (D_x is the x-demagnetizing factor) given by elementary magnetostatic arguments which are expected to be valid for a soft magnetic material such as Supermalloy.

A plot of transmission amplitude as a function of applied magnetic field for the Supermalloy disc is shown in Figure 3.3 for the usual FMAR configuration, i. e., the rf and the static fields were orthogonal. The peak occurred at a field H_a = 0.78 koe; this is close to the value $H_a = \frac{\omega}{\gamma} - 4\pi M_s$ = 0.76 koe predicted by theory, neglecting magnetic damping. The maximum shown in Figure 3.3 corresponded to a transmission amplitude ratio of 2.8×10^{-5} or a power ratio of -91 db. This power ratio is the quotient of the power reaching the microwave receiver and the power incident upon the transmitter cavity: it therefore depends

---

2. We can be certain that the transmission spikes near zero field for the parallel-parallel configuration, as well as the transmission dip shown in Figure 3.3, were due to domain walls because both of these transmission features displayed a small but significant hysteresis when the external field was cycled from large positive to negative values. The peak positions were shifted approximately 5 oe. A transmission peak of similar origin has been observed in Metglas 2826 for the parallel-parallel configuration (Cochran et al., 1977b). Metglas 2826 ($Fe_{40}Ni_{40}P_{14}B_6$, an amorphous ferromagnet) is a trade name of the Allied Chemical Corporation, Morristown, N. J.

upon geometrical factors such as specimen apertures as well as upon the cavity quality factors. The measured power ratio agreed, within a factor of 2, with that calculated by Cochran et al. (1977a) taking the specimen geometry into account.

The field variation of transmission amplitude for both the parallel-parallel and parallel-perpendicular configurations are shown superposed and normalized to the same peak amplitude in Figure 3.4. It should be borne in mind that the peak amplitudes differ in strength by approximately 600. Apart from the zero field signals, these transmission curves are sufficiently similar as to leave no doubt that the parallel-parallel signal was just the usual FMAR signal excited by a small component of the rf field orthogonal to the magnetization. This conclusion is reinforced by the observation that when the active area of the specimen was increased from 2 mm^2 to 10 mm^2 the ratio of the parallel-perpendicular to parallel-parallel amplitude[3] decreased to 25. We do not know why the parallel-parallel transmission peak is a distorted version of the FMAR peak - a similar distortion and shift toward higher fields has also been observed for specimens of the amorphous metal alloy Metglas 2826. It may be an effect due to surface roughness. Small surface irregularities would be expected to give regions within the skin-depth where the local magnetization would deviate from

3. It should be noted that the difference between these ratios is probably due in part to the difference in shielding techniques. In the second case, instead of the evaporated gold layer, the sample was shielded by a free-standing copper diaphragm. Thus there was probably some propagation of microwaves parallel to the sample surface behind the diaphragm. However, we know independently that there was no leakage.

the direction of the bulk saturation magnetization. Alternatively, it may be that the presence of a thick (0.3 mm) copper diaphragm (See Figure 3.1) caused a small imhomogeneity in the rf magnetic field.

Although I observed nothing in the transmission through the 40μm Supermalloy specimen for the parallel-parallel configuration which resembled the transmission signals reported for iron and nickel by Lieu and Alexandrakis (1975), it could be argued a) that their observations were specifically concerned with iron and nickel, and that b) the ratio of specimen thickness to skin-depth for the Supermalloy specimen was too large to reveal their effect. In order to duplicate their experiment as closely as possible I there fore also measured transmission through a polycrystalline nickel foil for which $d/\delta = 7.9$, a value close to that used by Lieu and Alexandrakis[4] ($d/\delta = 6.8$). The results of the experiment are shown in Figure 3.5. Transmission for the parallel-perpendicular configuration, the usual FMAR configuration, is shown on the same scale as the transmission for the parallel-parallel configuration. The peak signal at FMAR corresponded to an amplitude ratio of 3.3×10^{-6}, or a power ratio of -110 db. The field independent plateau in the parallel-parallel configuration corresponded to an amplitude ratio of 5.8×10^{-7}. An estimate of this transmission ratio for a non-magnetic metal having the DC resistivity of nickel, and

4. Lieu and Alexandrakis used $\delta = (\rho c^2/4\pi\omega)^{\frac{1}{2}} = 3.2$ μm; they calculated the skin-depth using $\rho = 19$ μΩcm, a value approximately 2½ times larger than the DC resistivity of nickel.

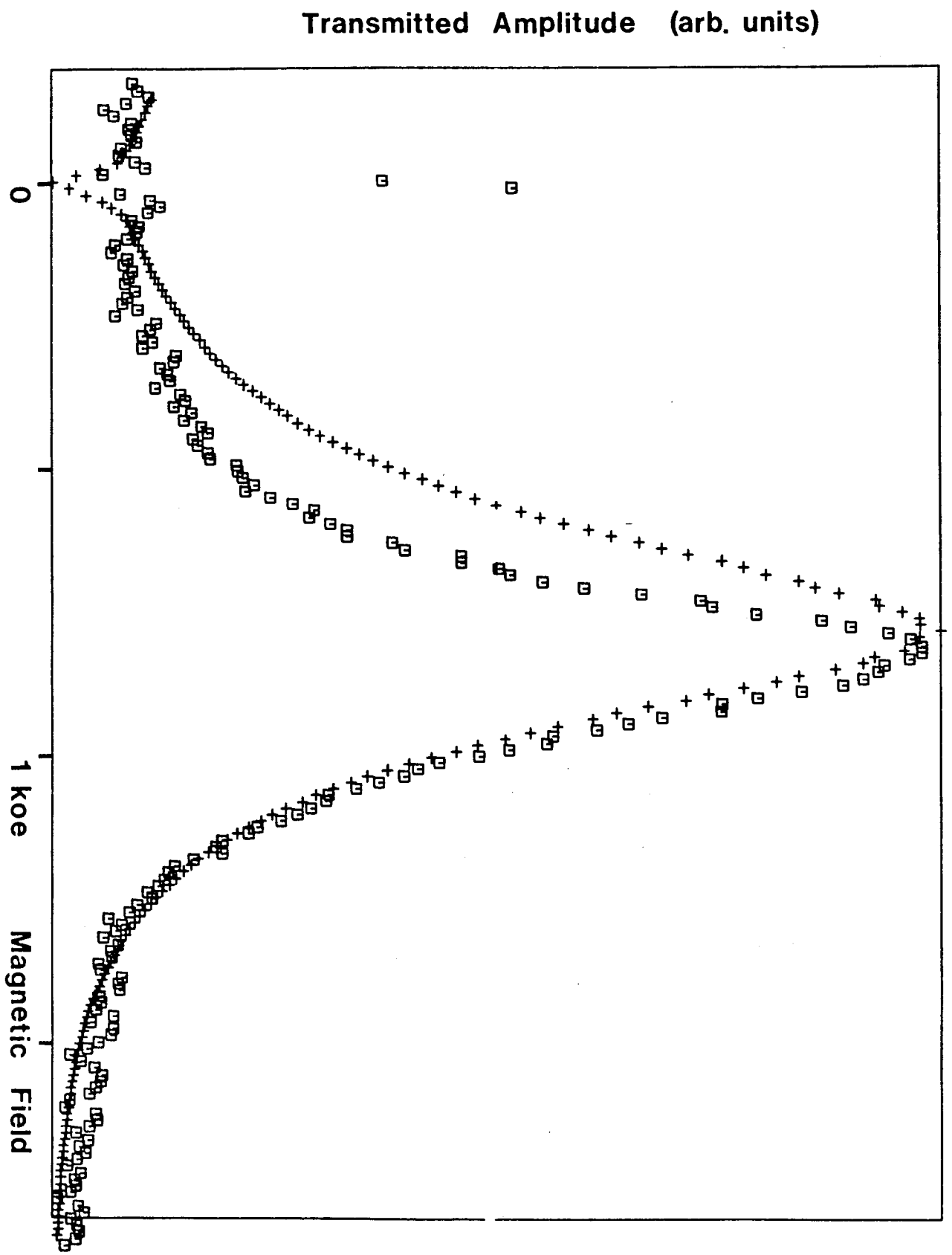
Transmitted Amplitude (arb. units)
0
1 koe
Magnetic Field

Figure 3.4 The two orthogonal transmission phases of Figure 3.2 measured for the Supermalloy disc using the parallel-parallel configuration have been combined to give transmission amplitude vs. magnetic field (□). These data have been superposed on the FMAR transmission signal of Figure 3.3 (+). These transmission curves have been normalized to the same peak transmission amplitude: the FMAR signal is approximately 600 times larger in amplitude than the parallel-parallel signal.

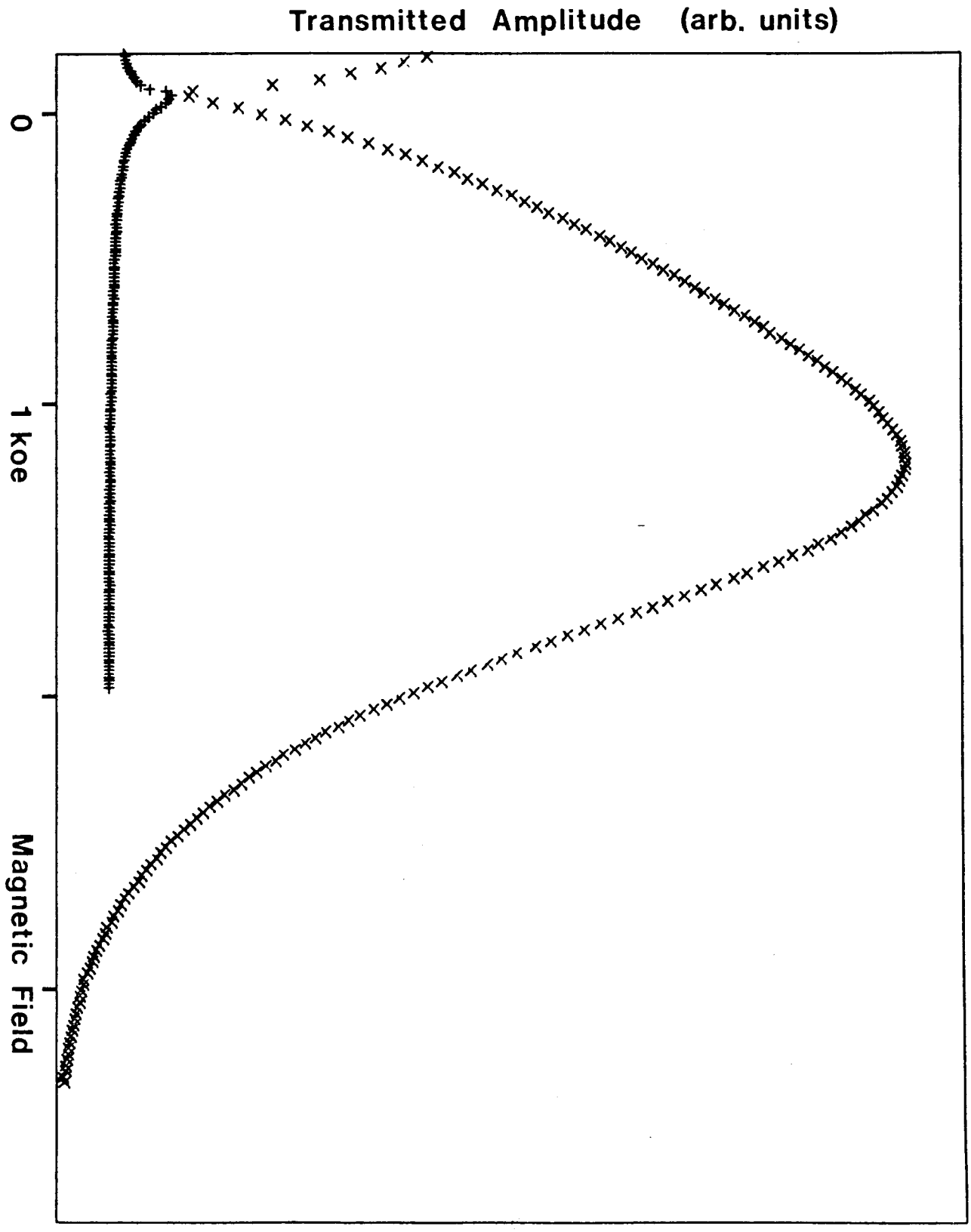
Transmitted Amplitude (arb. units)
0
1 koe
Magnetic Field

Figure 3.5 Transmission amplitude vs. decreasing magnetic field for a 7.2 μm thick polycrystalline nickel foil. (x): The usual FMAR configuration having rf and static fields orthogonal. The peak transmitted power was -110 db, and occurred at 1.2 koe. (+): The parallel-parallel configuration in which the rf and static fields were parallel. Both curves are plotted on the same scale.

taking the cavity quality factors and active area of the specimens into account as described by Cochran et al. (1977a), gave 5×10^{-7}. This agreement between the calculated and observed signal strength is strong evidence that the bulk of the signal observed for the parallel-parallel configuration was due to the ordinary skin-depth mode which is expected to be excited in the metal when the rf and static fields are parallel. The transmission peak near zero field was due to ferromagnetic domain boundaries as evidenced by the fact that it exhibited hysteresis. The displacement between transmission peaks due to hysteresis was approximately 100 oe. Domain wall effects occurred over a relatively large field interval in the nickel specimen because of magneto-crystalline anisotropy coupled with the polycrystalline nature of the specimen.

DISCUSSION

Apart from a field interval near zero, our observations on the transmission through a nickel foil for the parallel-parallel configuration are in agreement with the observations reported by Lieu and Alexandrakis, namely a field independent signal. The amplitude of this signal for both sets of data is consistent with the hypothesis that it is simply due to the ordinary electromagnetic wave which we expect to be excited in a ferromagnetic metal when the rf and static magnetic fields are parallel. We did not observe this background signal in our experiment on Supermalloy because the specimen was twice as thick in terms of skin-depths as was the nickel specimen (See Table 3.I). This was sufficient to cause the electromagnetic wave to be attenuated

to an unobservably small level.

Near zero field we observed an enhanced transmission (See the lower curve of Figure 3.5) which was clearly due to ferromagnetic domain wall motion because the peak occurred at different fields depending upon the history of the magnetic field cycle. Lieu and Alexandrakis observed an attenuated transmission near zero field. Possibly this attenuation near zero field is an effect due to the motion of superficial domain walls. It can be argued that the presence of domain walls within the specimen may either diminish or increase transmission depending upon their location and orientation. Those confined to the sample surface would tend to shield its interior from microwaves. Consider, however, domain walls which extend through the specimen. It is the latter type of domain wall which is responsible for enhanced transmission near zero field. Thus the different results reported by our two groups could be due to differences in samples which favored the dominance of one sort of domain wall over the other.

A more detailed investigation of the zero-field transmission anomaly is currently underway in our laboratory using materials for which the domain structure can be well-characterized.

Can you picture yourself,
So limitless and free,
Desperately in need
Of some stranger's hand?
"The End"
The Doors

Chapter 4

Conclusion

I have pointed out the error in the theory of Lieu and Alexandrakis. In the realm of saturated magnetization, their data can be explained in terms of the linear theory. Where their data differs qualitatively from mine (i. e. in the region below saturation) the difference may well be due to differences in sample preparation which influenced domain wall motion.

The effect they observe is very probably the non-magnetic (field independent) mode (of equation 1.8), but modulated by domain wall motion at fields for which the sample is divided into magnetic domains.

I must add that, excepting only their experience, I know of no reason to expect the conductivity at 24 GHz to be different (especially so markedly) from the DC conductivity. I have fitted the data in Figure 3.3 without resort to this. Their use of a conductivity differing by a factor of 2½ (as noted in footnote 4 of the last chapter) from the DC value seems excessive.

APPENDIX

NONLINEAR EFFECTS IN FERROMAGNETIC METALS*

O.L.S. Lieu and G.C. Alexandrakis
Physics Department, University of Miami
Coral Gables, Florida 33124

ABSTRACT

A nonlinear theory of ferromagnetic transmission resonance in the case in which the static and microwave fields are mutually parallel and parallel to the sample surface is outlined. Its predictions are compared to experimental results obtained for iron and nickel. The theory predicts strong subharmonic generation of possible practical use.

THEORY

The effects described here are strictly ferromagnetic. Experimentally they are not observed in paramagnetic metals.[1] Assume the sample is in foil form of thickness d and is made to form the common wall of two identical microwave cavities. One cavity is used to store the incident microwaves of frequency ω_0 and the other to collect the power transmitted through the sample. Take the sample to lie on the xz-plane. The microwaves propagate along the y-axis. Both the applied static and microwave fields are along the z-axis.[1,2]

The Bloch-Bloembergen and Maxwell equations for this problem are written as:

$$\left.\begin{aligned}
&\frac{\partial M_x}{\partial t} = \gamma(M_y H_a - M_s H_y) - \frac{2\gamma A}{M_s}\nabla^2 M_y - \frac{M_x}{\tau}\\
&\frac{\partial M_y}{\partial t} = \gamma(M_s H_x - M_x H_a) + \frac{2\gamma A}{M_s}\nabla^2 M_x - \frac{M_y}{\tau}\\
&\frac{\partial M_z}{\partial t} = \gamma(M_x H_y - M_y H_x) + \frac{2\gamma A}{M_s^2}(M_x\nabla^2 M_y - M_y\nabla^2 M_x) - \frac{M_z}{T_1}\\
&\vec{\nabla}\cdot(\vec{H}+4\pi\vec{M}) = 0\\
&\vec{\nabla}\times\vec{H} = \frac{4\pi\sigma}{c}\vec{E}\\
&\vec{\nabla}\times\vec{E} = -\frac{1}{c}\frac{\partial}{\partial t}(\vec{H}+4\pi\vec{M})
\end{aligned}\right\} \quad (1)$$

Here $\vec{H} = (H_x, H_y, H_a+H_z)$, $\vec{M} = (M_x, M_y, M_s+M_z)$ where H_a is the applied static field, M_s is the saturation magnetization, $H_{x,y,z}$ and $M_{x,y,z}$ are the high frequency components of the fields. Other symbols have their standard meanings.

Assume the plane wave solutions $H_{x,y} = h_\lambda^{x,y}\, e^{-(\lambda y + i\omega t)}$, $M_{x,y} = m^{x,y}\, e^{-(\lambda y + i\omega t)}$ for the transverse components of Eqs. (1). We obtain the secular equation for the propagation constant λ by using the transverse component equations from Eqs. (1), to be

$$\lambda^6 + a_2\lambda^4 + a_1\lambda^2 + a_0 = 0 \quad (2)$$

where

$$a_2 = \frac{2i}{\delta^2} - \frac{(\omega_B+\omega_H)}{\Lambda M_s},\quad a_1 = \frac{\vartheta^2+\omega_B\omega_H}{\Lambda^2 M_s^2} - \frac{4i\,\omega_B}{\delta^2\Lambda M_s},\quad a_0 = \frac{2i}{\delta^2}\frac{(\vartheta^2+\omega_B^2)}{\Lambda^2 M_s^2}$$

$$\Lambda = \frac{2\gamma A}{M_s^2},\quad \vartheta = \frac{1}{\tau} - i\omega,\quad \delta = \frac{c}{\sqrt{2\pi\omega\sigma}}\ (\text{skin depth})$$

$$\omega_H = \gamma H_a,\quad \omega_M = 4\pi\gamma M_s,\quad \omega_B = \omega_H + \omega_M$$

Equation (2) is cubic in λ^2, the roots are $\pm\lambda_1$, $\pm\lambda_2$, $\pm\lambda_3$ which can be expressed in terms of a_0, a_1, a_2 analytically. They give the wave propagation along $+\hat{y}$ and $-\hat{y}$.

We now write

$$H_x=\sum_j (A_j e^{-\lambda_j y}+B_j e^{\lambda_j y})e^{-i\omega t} \quad (j=1,2,3) \tag{3}$$

and similar expressions for M_x, M_y, H_y where A_j and B_j are the amplitudes to be determined by boundary conditions. Using these expressions of the transverse fields in the longitudinal components of (1) we solve for H_z. The solution is

$$H_z=\sum_{j,\ell}[\alpha_{j\ell}(A_j A_\ell e^{-a_{j\ell}y}+B_j B_\ell e^{a_{j\ell}y})+\beta_{j\ell}(A_j B_\ell e^{-b_{j\ell}y}+B_j A_\ell e^{b_{j\ell}y})]e^{-i2\omega t} \tag{4}$$

where

$$\alpha_{j\ell}=\lambda_j+\lambda_\ell\ ,\ b_{j\ell}=\lambda_j-\lambda_\ell\ ,\ \alpha_{j\ell}=\frac{(-i8\pi\omega c_1)\epsilon_{j\ell}}{(\kappa_0^2 a_{j\ell}^2+i2\omega)}\ ,\ \beta_{j\ell}=\frac{(-i8\pi\omega c_1)\epsilon_{j\ell}}{(\kappa_0^2 b_{j\ell}^2+i2\omega)}$$

$$\kappa_0^2=\frac{\omega^2}{4\pi\sigma}\ ,\ c_1=\frac{\tau_1(1+i2\omega\tau_1)}{(1+4\omega^2\tau_1^2)}\ ,\ \epsilon_{j\ell}=\frac{-1}{2}\left[\frac{\gamma}{4\pi}(\xi_j\eta_\ell+\eta_\ell)+\frac{\Lambda}{(4\pi)^2}\xi_j\eta_\ell(\lambda_j^2-\lambda_\ell^2)\right]$$

$$\xi_j=-(\lambda^2+2i\zeta^2)/(2i\zeta^2)\ ,\ \eta_j=\frac{\partial\xi_j}{(\omega_B-\Lambda M_s\lambda_j^2)} \quad (j,\ell=1,2,3)$$

Notice that the field transmitted along the z-axis is at the applied frequency $\omega_0=2\omega$ whereas the one transmitted along the x-axis has the frequency $\omega=\omega_0/2$.

We now begin to solve the boundary value problem for the transmitted fields. The boundary conditions are (a) the tangential components of $\vec{H}$ and $\vec{E}$ are continuous across the sample surfaces at y=0 and y=d, (b) Kittel's boundary condition for the transverse magnetization, i.e. $M_x=0$ at y=o,d. We arrange the boundary conditions in two groups. The first group which contains the boundary conditions on H_x, E_z and M_x, is written in matrix form as

$$\left.\begin{aligned}
&M_1\begin{pmatrix}A_1\\B_1\end{pmatrix}+M_2\begin{pmatrix}A_2\\B_2\end{pmatrix}+M_3\begin{pmatrix}A_3\\B_3\end{pmatrix}=\begin{pmatrix}r\\t\end{pmatrix}\\
&\lambda_1 N_1\begin{pmatrix}A_1\\B_1\end{pmatrix}+\lambda_2 N_2\begin{pmatrix}A_2\\B_2\end{pmatrix}+\lambda_3 N_3\begin{pmatrix}A_3\\B_3\end{pmatrix}=\frac{4\pi\sigma}{c}\begin{pmatrix}-r\\t\end{pmatrix}\\
&\xi_1 M_1\begin{pmatrix}A_1\\B_1\end{pmatrix}+\xi_2 M_2\begin{pmatrix}A_2\\B_2\end{pmatrix}+\xi_3 M_3\begin{pmatrix}A_3\\B_3\end{pmatrix}=\begin{pmatrix}0\\0\end{pmatrix}
\end{aligned}\right\} \tag{5}$$

where

$$M_j=\begin{pmatrix}1 & 1\\ e^{-\lambda_j d} & e^{\lambda_j d}\end{pmatrix},\ N_j=\begin{pmatrix}1 & -1\\ e^{-\lambda_j d} & -e^{\lambda_j d}\end{pmatrix},\ r=H_{rx}\ ,\ t=H_{tx}e^{ik_0' d}\ ,\ K_0'=\frac{\omega}{c}$$

H_{rx} and H_{tx} are the reflected and transmitted amplitudes along the x-axis.

From (5) we have

$$\left.\begin{aligned}
\begin{pmatrix}A_1\\B_1\end{pmatrix}&=-G^{-1}(\xi_3\lambda_2 P_2-\xi_2\lambda_3 P_3)\begin{pmatrix}r\\t\end{pmatrix}+\frac{4\pi\sigma}{c}(\xi_3-\xi_2)G^{-1}\begin{pmatrix}-r\\t\end{pmatrix}\ .\\
\begin{pmatrix}A_2\\B_2\end{pmatrix}&=\left[\frac{\xi_3 M_2^{-1}}{(\xi_3-\xi_2)}+\frac{(\xi_3-\xi_1)}{(\xi_3-\xi_2)}M_2^{-1}M_1 G^{-1}(\xi_3\lambda_2 P_2-\xi_2\lambda_3 P_3)\right]\begin{pmatrix}r\\t\end{pmatrix}\\
&\qquad -\frac{4\pi\sigma}{c}(\xi_3-\xi_1)M_2^{-1}M_1 G^{-1}\begin{pmatrix}-r\\t\end{pmatrix}\\
\begin{pmatrix}A_3\\B_3\end{pmatrix}&=\left[\frac{-\xi_2 M_3^{-1}}{(\xi_3-\xi_2)}+\frac{(\xi_1-\xi_2)}{(\xi_3-\xi_2)}M_3^{-1}M_1 G^{-1}(\xi_3\lambda_2 P_2-\xi_2\lambda_3 P_3)\right]\begin{pmatrix}r\\t\end{pmatrix}\\
&\qquad +\frac{4\pi\sigma}{c}(\xi_2-\xi_1)M_3^{-1}M_1 G^{-1}\begin{pmatrix}-r\\t\end{pmatrix}
\end{aligned}\right\} \tag{6}$$

where

$$G=(\xi_3-\xi_2)\lambda_1 N_1+[(\xi_2-\xi_1)\lambda_3 P_3+(\xi_1-\xi_3)\lambda_2 P_2]M_1\ ,\ P_j=N_j M_j^{-1}$$

We can write (6) as

$$\begin{pmatrix}A_j\\B_j\end{pmatrix}=\begin{pmatrix}\Delta_j & \theta_j\\ \Lambda_j & \varphi_j\end{pmatrix}\begin{pmatrix}r\\t\end{pmatrix} \quad (j=1,2,3) \tag{7}$$

The second group of boundary conditions which contains the ones on H_z, E_x gives the following equations

$$\left.\begin{aligned} r^2\psi_1(o) + t^2\psi_2(o) + rt\,\psi_3(o) &= H_{rf} + H_{rz} \\ r^2\psi_1(d) + t^2\psi_2(d) + rt\,\psi_3(d) &= H_{tz}\, e^{ik_o d} \\ r^2\phi_1(o) + t^2\phi_2(o) + rt\,\phi_3(o) &= -H_{rf} + H_{rz} \\ r^2\phi_1(d) + t^2\phi_2(d) + rt\,\phi_3(d) &= -H_{tz}\, e^{ik_o d} \end{aligned}\right\} \qquad (8)$$

where

$$\psi_1(\gamma) = \sum_{j,\ell}\left\{\alpha_{j\ell}(\Delta_j\Delta_\ell e^{-a_{j\ell}\gamma} + \Lambda_j\Lambda_\ell e^{a_{j\ell}\gamma}) + \beta_{j\ell}(\Delta_j\Lambda_\ell e^{-b_{j\ell}\gamma} + \Lambda_j\Delta_\ell e^{b_{j\ell}\gamma})\right\}$$

$$\psi_2(\gamma) = \sum_{j,\ell}\left\{\alpha_{j\ell}(\theta_j\theta_\ell e^{-a_{j\ell}\gamma} + \varphi_j\varphi_\ell e^{a_{j\ell}\gamma}) + \beta_{j\ell}(\theta_j\varphi_\ell e^{-b_{j\ell}\gamma} + \varphi_j\theta_\ell e^{b_{j\ell}\gamma})\right\}$$

$$\psi_3(\gamma) = \sum_{j,\ell}\left\{\alpha_{j\ell}[(\Delta_j\theta_\ell + \theta_j\Delta_\ell)e^{-a_{j\ell}\gamma} + (\Lambda_j\varphi_\ell + \varphi_j\Lambda_\ell)e^{a_{j\ell}\gamma}] + \beta_{j\ell}[(\Delta_j\varphi_\ell + \theta_j\Lambda_\ell)e^{-b_{j\ell}\gamma} + (\Lambda_j\theta_\ell + \varphi_j\Delta_\ell)e^{b_{j\ell}\gamma}]\right\}$$

$\phi_j(\gamma) = \frac{c}{4\pi\sigma}\frac{d\psi_j}{d\gamma}$, $k_o = \frac{\omega_o}{c}$, H_{rf} is the incident microwave amplitude, H_{rz} and H_{tz} are the reflected and transmitted amplitudes along the z-axis.

The H_{tz} and H_{tx} are obtained from (8) to be

$$H_{tz} = H_{rf}\, e^{-ik_o d}\, Z_{(\pm)} \qquad (9)$$

$$H_{tx} = \sqrt{2H_{rf}}\, e^{-ik_o' d}\, X_{(\pm)} \qquad (10)$$

where

$$Z_{(\pm)} = \frac{\pi_1\Delta^2_{(\pm)} + \pi_2 + \pi_3\Delta_{(\pm)}}{\Gamma_1\Delta^2_{(\pm)} + \Gamma_2 + \Gamma_3\Delta_{(\pm)}}, \quad X_{(\pm)} = \frac{1}{\sqrt{\Gamma_1\Delta^2_{(\pm)} + \Gamma_2 + \Gamma_3\Delta_{(\pm)}}}$$

$$\Delta_{(\pm)} = \left(-\Omega_3 \pm \sqrt{\Omega_3^2 - 4\Omega_1\Omega_2}\right)/2\Omega_1$$

$$\Gamma_j = \psi_j(o) - \phi_j(o), \quad \Omega_j = \psi_j(d) + \phi_j(d), \quad \pi_j = \psi_j(d) - \phi_j(d)$$

The theoretical signal is

$$H_T = Re\left\{A\, e^{-i(k_o d + \phi)}\, Z_{(\pm)}\right\}$$

where A is the amplification factor and ϕ is an arbitrary phase introduced by the apparatus.

The power transmitted along the z-axis is then proportional to $|Z_{(\pm)}|^2$ while the one transmitted along the x-axis is proportional to $|X_{(\pm)}|^2$.

DISSCUSSION

In Fig. 1(a) and 1(d) we have plotted the experimental transmitted amplitudes along the z-direction for a 18μm thick Fe foil and a 10 μm thick Ni sample, at room temperature. The frequency of H_{zt} which is the same as the excitation frequency is close to ν_0 = 9.2 GHz. The theoretical results for $|H_{zt}|$ for Fe and Ni correspondingly are plotted in Fig. 1(b) and 1(e). The calculated $|H_{xt}|$ values for Fe and Ni are shown in Fig. 1(c) and 1(f). As was indicated above the H_{xt} field has half the applied frequency.

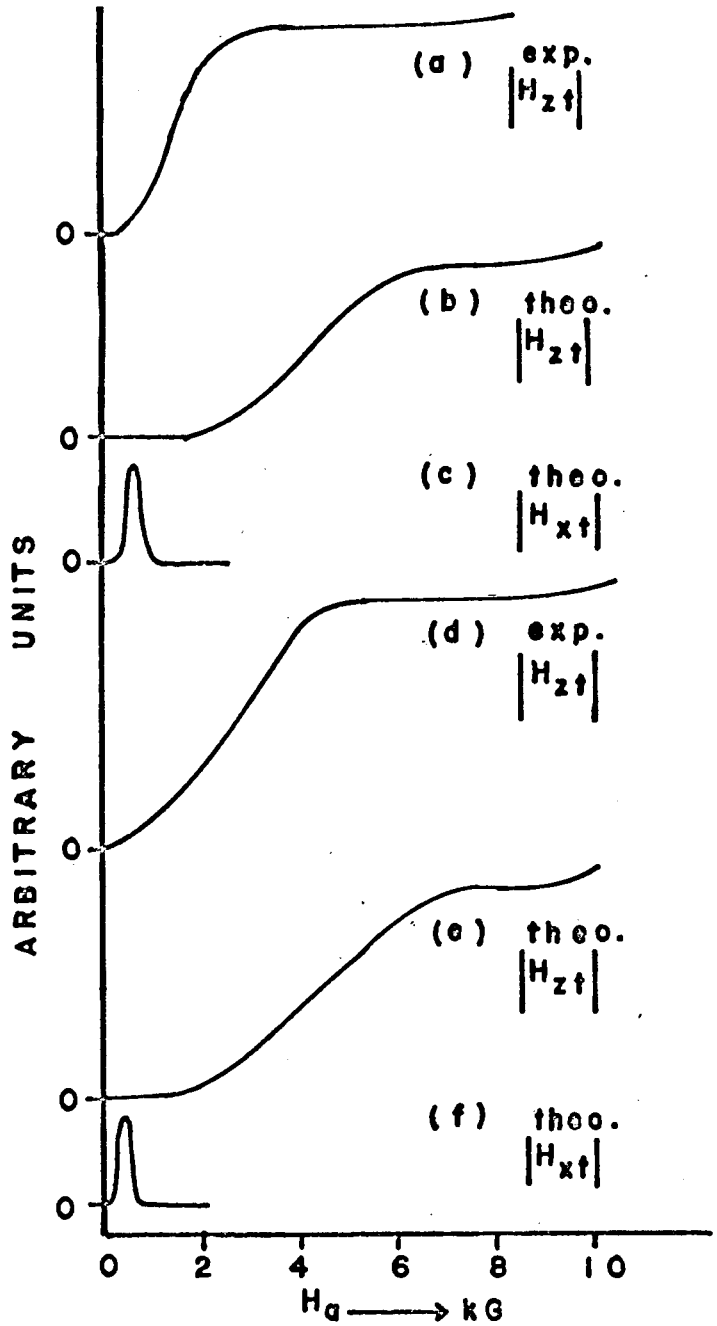

FIG. 1 (a) experimental, (b), (c) theoretical results for Fe. (d) experimental, (e), (f) theoretical results for Ni. Parameter values are given in text.

The parameter values used for the Fe plots are: M_s = 1707 G, g = 2.05, $\tau = 1.0 \times 10^{-10}$ sec, $T_1 = 1 \times 10^{-10}$ sec, δ = 5 μm and $A = 2.5 \times 10^{-6}$ ergs/cm. For Ni we used: M_s = 485, g = 2.2, $\tau = 1.0 \times 10^{-10}$, $T_1 = 1.0 \times 10^{-10}$, δ = 3.2μm and $A = .9 \times 10^{-6}$ ergs/cm. The values we used for δ which in our theory enters for the frequency $\nu_o/2$ are 50% larger than their suggested values from static resistivity data. This is in accordance with our past experience in metals. The A value for Ni used here is slightly larger than the published value[3] of $A = .75 \times 10^{-6}$ ergs/cm. The A value for Fe is the same as the published value.[3]

The calculated values for the $|H_{zt}|$'s are about one order of magnitude smaller than their experimental values. The $|H_{xt}|$'s are about two order of magnitude stronger than the $|H_{zt}|$'s. This is generally consistent with the fact that the H_{xt}'s have a larger skin depth than the H_{zt}'s.

In summary, what appears to be the case in the phenomena described here is that at low static field values most of the incident power along the z-axis, is pumped into the $H_{x,y}$ components through excitation of transverse spin waves, reminiscent of parallel pumping in insulators.[4] However at high static field values most of the power is retained by the H_{zt} component after allowing for normal attenuation in the metal.

We have observed the H_{zt} transmission resonance phenomenon in practically all ferromagnetic metals. Besides δ,on which all microwave propagations in metals have a strong dependence, the calculated H_{zt}'s are very strongly dependent on A contrary to other linear bulk resonance effects.[5] Thus the nonlinearity is predominantly dependant on A. We plan to fit the experimental results with the theory to try to establish the temperature dependence of the exchange constant. The predicted subharmonic generation might have practical use in special cases. Thin films will have to be used, although even then this method could not compete with the present harmonic generating diodes in most cases. We are presently preparing to detect the $|H_{xt}|$ and assess its usefulness.

We wish to thank Dr. M.A. Huerta for helpful suggestions regarding the calculations.

REFERENCES

*Work supported by the National Science Foundation.

1. G.C. Alexandrakis, O. Horan, T.R. Carver, and C.N. Manicopoulos, Phys. Rev. Lett. 25, 1758 (1970).
2. O.L.S. Lieu and G.C. Alexandrakis and M.A. Huerta, to be published.
3. B.E. Argyle, S. Charap, and E.W. Pugh, Phys. Rev. 132, 2051 (1963); F. Keffer, Handbuck der Physik XVIII/2, 30 (Springer-Verlag, Berlin, 1966); C. Herring, Rado and Suhl, Magnetism IV, Academic Press, New York, 1966, p. 357.
4. F.R. Morgenthaler, J. Appl. Phys. 31, 95S (1960); E. Schlomann, J.J. Green, and U. Milano, J. Appl. Phys. 31, 386S (1960); C. Kittel, Quantum Theory of Solids, (Wiley, New York, 1964),p. 69; M. Sparks, Ferromagnetic-Relaxation Theory, (McGraw-Hill, New York, 1964) contains an extensive bibliography on nonlinear effects in insulators.
5. O. Horan, G.C. Alexandrakis, and C.N. Manicopoulos, Phys. Rev. Lett. 25, 246 (1970).

BIBLIOGRAPHY

Alexandrakis, G. C., Horan, O., Carver, T. R., and Manicopoulos, C. N. 1970. Phys. Rev. Lett. 25, 1758.

Ament, W. S. and Rado, G. T. 1955. Phys. Rev. 97, 1558.

Argyres, P. and Kittel, C. 1953. Acta Met. 1, 241.

Bloembergen, N. 1950. Phys. Rev. 78, 572.

Cochran, J. F., Heinrich, B., and Dewar, G. 1977(a). To be published in the Canadian Journal of Physics.

Cochran, J. F., Heinrich, B., and Baartman, R. 1977(b). Proceedings ICM 76. To be published in Physica B (Neth).

Dewar, G., Heinrich, B., and Cochran, J. F. 1977. To be published in the Canadian Journal of Physics.

Heinrich, B. and Meshcheryakov, V. F. 1969. ZhETF Pis. Red. 9, 618. JETP Lett. 9, 378 (1969).

Heinrich, B. and Meshcheryakov, V. F. 1970. ZhETF 59, 424. Soviet Phys. JETP 32, 232 (1971).

Herring, C. and Kittel, C. 1951. Phys. Rev. 81, 869.

Hill, D. J. and Edwards, D. M. 1973. J. Phys. F (GB) 3, L162.

Kittel, C. 1971. Introduction to Solid State Physics. 4th ed. (Wiley, New York).

Kurn, A., Cochran, J. F., and Hienrich, B. 1976. Can. J. Phys. 54, 1083.

Lieu, O. L. S., and Alexandrakis, G. C. 1975. AIP Conf. Proc. 24, 512, ed. by C. D. Graham, G. H. Lander, and J. J. Rhyne (AIP, New York).

Messiah, Albert 1962. Quantum Mechanics. (North-Holland, Amsterdam).

Rado, G. T. and Weertman, J. R. 1959. J. Phys. Chem. Solids 11, 315.

Schlomann, E., Green, J. J., and Milano, U. 1960. J. Appl. Phys. 31, 386S.

Ziman, J. M. 1972. Principles of the Theory of Solids. 2nd ed. (Cambridge University Press, London).